Electronic transport properties of NbC(C)-C nanocomposites

D. Li, W. F. Li, S. Ma, and Z. D. Zhang

Shenyang National Laboratory for Materials Science, Institute of Metal Research and International Center for Materials Physics,
Chinese Academy of Sciences, 72 Wenhua Road, Shenyang 110016, People's Republic of China

We report the electronic transport properties of a composite system comprising zero dimensional superconducting NbC(C) nanocapsules and carbon nanofiber matrix. DC susceptibility measurements of the nanocomposite indicate that the critical temperature (T_C) of NbC nanocrystals is 10.7 K. The temperature dependence of electrical resistivity of the specimen pellet follows the Mott's $T^{-1/4}$ law in a temperature range between T_C of NbC and 300 K, owing to a strong degree of structural disorder in the carbon matrix. Below the T_C of NbC, when the change of its electrostatic energy ΔE is far greater than the thermal energy, an electron will be localized on an isolated NbC nanocrystal at very low temperatures, leading to "Coulomb Blockade." As a result, a collective behavior of the single-electron tunneling effect takes place in a three-dimensional granular superconductors' network composed of the NbC/carbon/NbC tunneling junctions. The superconducting gap of NbC crystals is not found in the current-voltage curves, due to the suppression of surface superconductivity through the contact between NbC and carbon shells.

PACS number(s): 73.23.Hk, 72.80.Tm, 72.15.Rn

The electrical conduction mechanisms in composite systems comprising an intricate network of conducting and insulating phases are usually attributed to percolation in a continuous conducting network[1] and/or tunneling[2–4] between isolated conducting particles (grains, crystallites, etc.). A considerable finite conductivity was observed in the dielectric regime,[5,6] where a metal continuum was absent. This conductivity was ascribed to interparticle tunneling.[2,5,7] More recently, the question of tunneling and percolation in these systems below the percolation threshold was investigated by Toker *et al.*[8] and Balberg *et al.*[9] On the other hand, superconductivity in granular mixture films was studied, both experimentally and theoretically, in the framework of the percolation theory.[10,11] It was demonstrated that for a random mixture of granular superconducting and insulating materials the superconductor (S)—insulator (I) transition occurs at the percolation threshold. The properties of nanocomposite materials depend not only on the properties of their individual parents but also on their morphology and interfacial characteristics. The reduction of the particle's size d could lead to dramatic changes of the physical behavior of superconductors, such as a huge enhancement on the critical field[12] and/or superconducting state of nanosized superconductors.[13–16] According to Kubo and co-workers,[17–20] the energy gap between the nearest neighboring energy level increases rapidly with decreasing the particle size of metal particles, thus the physical properties of metal particles would evidently differ from those of bulk materials. As the gap of the discreteness of the energy levels is larger than the thermal energy $k_B T$, quantum size effect becomes much more pronounced and surface effects play a more important role. For YC_2 single crystal encapsulated in a carbon nanocage[21,22] as one of the zero-dimensional (0D) superconductors, it was reported that its surface superconductivity was partially suppressed by the contact between YC_2 crystals and the innermost nanocages, owing to a proximity effect.[23] In our present work, the 0D superconducting NbC(C) nanocapsule-carbon nanofiber composite materials were prepared. Single-electron tunneling and variable range hopping (VRH) conductions were reported in the nanocomposite.

In our previous work,[24,25] a process of arc discharge was developed to fabricate magnetic nanocapsules with different types of shells and cores only by changing the atmosphere. The present work demonstrates that arc-discharging Nb in a CH_4 gas can synthesize the NbC-C nanocomposites. Argon (20 000 Pa) was introduced into an evacuated chamber (7 $\times 10^{-3}$ Pa). An arc between the cathode of a carbon rod with a diameter of 3 mm and the anode of a niobium ingot of 99.7% purity started to be stable with a current of 60 A. Then, CH_4 gas (4000 Pa) was rapidly introduced into the chamber. The mixed gas served as a reactant gas and a source of hydrogen plasma. When the current was maintained at 60 A and a potential sustaining in a range of 22–24 V between the cathode and the anode during the whole preparation, bulk Nb evaporated while CH_4 decomposed into C and [H]. Consequently, the NbC-C nanocomposites were condensed on the walls of the work chamber. Once the arc discharge process finished, residual gases were pumped out and Ar gas with a pressure 50 000 Pa was introduced for the passivation of the products. Deposits on the water-cooled walls of the chamber were collected and stored in air. The morphology and structure of the deposits were observed by a JEOL 2010EX transmission electron microscopy (TEM) operating at 200 kV. X-ray diffraction (XRD) pattern was recorded at room temperature in a $D/\max$-γA diffractometer with Cu K_α radiation under 50 kV and 250 mA. Carbon composition was determined by Raman spectrum. The dc susceptibility and magnetization curve were measured by employing a quantum design superconducting quantum interference device (SQUID) magnetometer. For resistivity measurements, the as-prepared NbC-C nanocomposites were pressed into a pellet in a diameter of 10 mm by using a 1.2 GPa axial pressure with a steel die. The temperature dependence of resistivity and the current-voltage characteristics of the NbC-C nanocomposites were studied using SQUID by the dc four-probe method.

The typical morphology of the NbC(C)-C nanocomposites fabricated in the methane (CH_4) atmosphere is shown in a TEM micrograph [Fig. 1(a)]. The contrast in the micrograph clearly shows that the NbC nanocrystals are well dispersed in
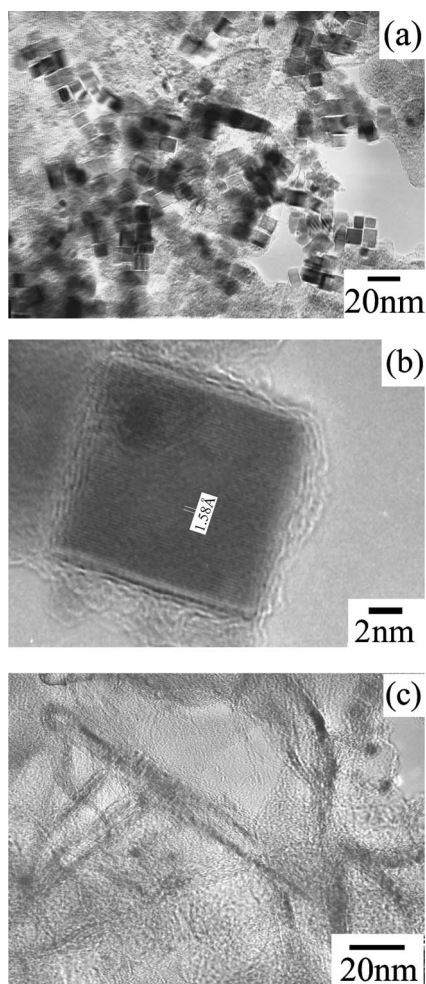
FIG. 1. (a) TEM image of the NbC-C nanocomposite showing NbC nanocrystals dispersed in carbon nanofiber matrix. HRTEM images of (b) a NbC(C) nanocapsule and (c) carbon nanofibers in both crystal and amorphous forms.

a matrix of carbon nanofibers and separated by carbon. The particle size of NbC nanocrystals is about 10 nm with a very narrow size distribution. Figure 1(b) exhibits a larger magnification of one NbC nanocrystal characterized by the 1.58 Å (220) lattice fringes, which clearly presents the core/shell structure of the NbC(C) nanocapsule. Figure 1(c) exhibits the image of the carbon nanofiber matrix in both crystal and amorphous forms. The XRD pattern of the nanocomposites could be indexed with cubic niobium carbide and carbon, as shown in Fig. 2, in good agreement with the TEM analysis. NbC nanocrystals with perfectly stoichiometric chemical composition were obtained during the arc discharging, thanks to a sufficient reaction between Nb vapors and excess C atoms coming from the decomposition of CH_4 and the evaporation of C cathode. It has been verified by dc magnetic susceptibility and electrical resistivity measurements, also in coincidence with the previous reports,[26–28] that high electrical conductivity and superconductivity could be observed only in the stoichiometric NbC specimens. XRD peaks of the carbon nanofibers shift to lower angles indicating a lattice expansion. Raman spectrum can be used to estimate the structural disorder in graphitic carbon samples.[29] As a result
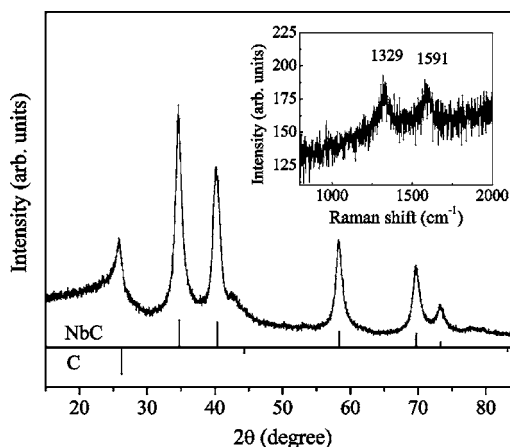
FIG. 2. X-ray diffraction pattern for the NbC-C nanocomposites prepared by discharging bulk Nb in Ar and CH_4. The inset shows the Raman spectrum at room temperature of the carbon nanofibers in the sample.

of Raman spectrum in the inset of Fig. 2, two characteristic Raman bands at 1329 cm^{-1} (D band) and 1591 cm^{-1} (G band) exist. The G band indicates the original graphite feature, but the D band suggests disorder features of the carbon structure.

Figure 3 shows the temperature dependence of electrical resistivity for the pellet of the NbC(C)-C nanocomposites, which is plotted in the form of resistivity ρ on a logarithmic scale against $T^{-1/4}$. The Raman spectrum, shown in the inset of Fig. 2, is suggestive of a high degree of disorder of the carbon nanofiber matrix, as indicated by the intensity of the D band relative to the G band. Consequently, electrons are strongly localized and the conductivity can be described by hopping conduction. In a three-dimensional case, the tem-
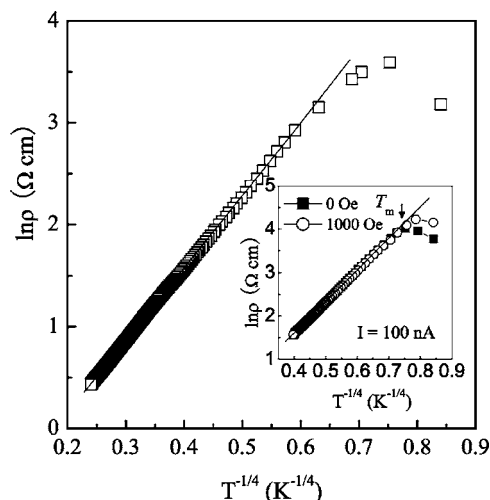
FIG. 3. Plot of the resistivity ρ on a logarithmic scale against $T^{-1/4}$ for the specimen pellet of the as-prepared NbC-C nanocomposite. The open square is for experimental data measured using a current of 100 μA. The inset represents the temperature dependence of resistivity between 2 and 40 K for the specimen pellet measured with a current of 100 nA at a zero field and a magnetic field of 1000 Oe, respectively. The solid lines show the linearity of the plots.
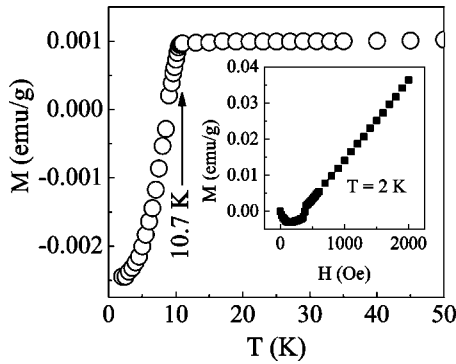
FIG. 4. Temperature dependence of dc susceptibility between 2 and 50 K for the nanocomposite measured at a magnetic field of 100 Oe. The inset shows the magnetization curve of the specimen measured at 2 K.

perature dependence of the hopping conductivity is derived by Mott as follows (Ref. 30):

$$\sigma(T) = \sigma_0 \exp\left(-\frac{T_0}{T}\right)^{1/4},$$

where σ_0 is a material constant and T_0 corresponds to a characteristic temperature of the system. A good linear fit between about the T_C of NbC and 300 K is satisfactory with the experimental data as represented in Fig. 3. It illustrates that the conductance of the specimen pellet is dominated by the carbon nanofibers matrix in terms of the VRH model. The carbon matrix can be treated as a semiconductor. According to Fig. 4, the temperature dependence of DC susceptibility of the nanocomposite in a temperature range 2 K $\leq T \leq 50$ K at a field of 100 Oe confirms that the critical temperature (T_C) of the NbC nanocrystals occurs at 10.7 K. Referring to the literature,[31] the coherence length of NbC is 24 nm, which is larger than the particle size (about 10 nm) of NbC nanocrystals. The T_C of the NbC nanocrystals is a little less than that of 11.5 K for a bulk NbC because the superconducting order parameter is suppressed. The magnetization at 2 K of the nanocomposite, shown in the inset of Fig. 4, points out that the superconductivity of the NbC nanocrystals disappeared as the applied field is about 380 Oe. The temperature dependence of resistivity for the specimen pellet measured at a zero field and a field of 1000 Oe, respectively, are represented in the inset of Fig. 3. As decreasing the temperature below the T_C of NbC, a deviation of the resistivity $\ln \rho(T)$ (obtained in a zero field) from the fitting line may result in single-electron tunneling between the superconducting NbC nanocrystals. When the applied magnetic field of 1000 Oe destroys the superconductivity of NbC nanocrystals, the electronic transport behavior of the specimen pellet is changed and again fallen into the VRH model with a negative temperature coefficient of electrical resistivity, leading to a positive magnetoresistance below the T_C of NbC. However, the resistivity $\ln \rho(T)$ of the carbon matrix at a field of 1000 Oe does not well keep the Mott's $T^{-1/4}$ law below a certain temperature (T_m) with no relationship to the superconductivity of NbC. It is the same as the previous report,[32] that the variable range hopping conduction could be affected
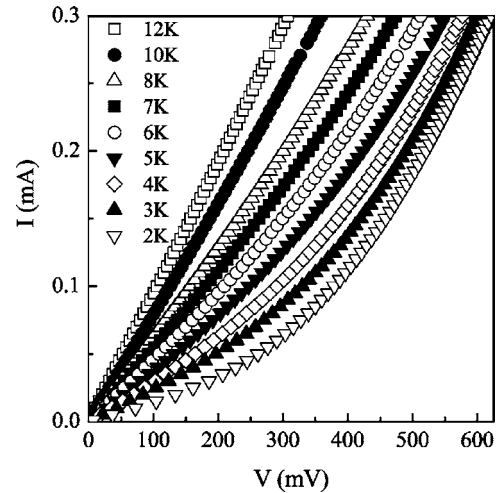
FIG. 5. Temperature dependence of I-V characteristics of the NbC/C/NbC tunneling junctions.

by a low magnetic field, which leads to a negative magnetoresistace.

Current-voltage (I-V) characteristics of the pellet of the NbC-C nanocomposite for different temperatures are shown in Fig. 5. Just below the T_C of NbC and down to 2 K, the I-V characteristics of the specimen pellet revealed a gradual growth of the tunneling current with increasing the potential bias. If a potential bias is applied to small isolated Sn nanoparticles imbedded in an insulating oxide film,[33] a current will flow due to electron tunneling. As an electron is brought on a very small isolated metal particle, the change of its charging energy $\Delta E = \frac{e^2}{2C}$ is far larger than the thermal energy $k_B T$ (e is the electron charge, C the capacitance, k_B the Boltzmann constant, and T the temperature) and the electronic transport is inhibited. The electrical capacitance of the unit cube C is about $0.66 \times 4\pi\varepsilon_0$.[34] In the case that an electron is added to a small isolated cubic NbC nanocrystal dispersed in a carbon dielectric matrix, the change of charging energy can be estimated by use of $\Delta E = \frac{e^2}{2 \times 0.66 d \times 4\pi\varepsilon_0 \varepsilon_r}$, where d is the length of side for the cube. Taking $\varepsilon_r = 2.5$ (estimated by carbon black) and $d = 10$ nm, ΔE is 7.06×10^{-21} J. The thermal energy is 1.38×10^{-22} J at 10 K and 2.76×10^{-23} J at 2 K, respectively. When ΔE is far greater than $k_B T$, an electron will be localized on the NbC nanocrystal and it is very hard to go from one nanocrystal to the other at very low temperatures. The suppression of the electronic transport between two of the nearest neighbor superconducting NbC nanocapslues is Coulomb Blockade. In the present system, the TEM [see Fig. 1(a)] reminds us that nanosized NbC/carbon/NbC junctionlike configurations are widely formed as the isolated cubic NbC nanocrystals are dispersed in the semiconducting carbon matrix and separated by carbon shells. As temperature decreases below the T_C of NbC, single-electron tunneling takes place, which leads to the gradual appearance of nonlinearity in the resistivity $\ln \rho(T)$ curve in Fig. 3 below the critical transition of NbC nanocrystals.

Of course, one would expect to see evidence of a superconducting gap in the I-V curves as shown in Fig. 5. In many cases, a gap is clearly present, such as the tunneling junction

of NbC-Pb thin films.[26] However, in the previous study on the YC$_2$(C) nanocapsules,[22] the contact of YC$_2$ nanocrystals with normal metal of the carbon shell could serve as a pair breaking mechanism, which locally enhances the effect of the magnetic field. It would result in a partial suppression of the surface superconductivity as pointed out by Tinkham.[35] As shown in the high resolution TEM (HRTEM) image [Fig. 1(b)], the NbC(C) nanocapsules with a structural feature almost the same as YC$_2$(C) nanocapsules should also support the standpoint above. Furthermore, the previous study of single-electron tunneling in point-contact tunnel junctions between a tungsten tip and a Yba$_2$Cu$_3$O$_{7-\delta}$ surface[36] indicated that when the surface layer of the superconductor is not superconducting, a gap in the I-V curve would be invisible. This explains why there is no sharp increase of the tunneling current corresponding to the superconducting gap of NbC observed in the I-V characteristics in Fig. 5.

The microstructure in our system could be represented as a zero-dimensional superconductors' tunneling network composed of the S-I-S (NbC/carbon/NbC) tunneling junctions. As well, the tunneling junctions are slightly different because the thickness of the carbon shell and the size of the NbC nanocrystals are slightly variable. It should be noted that the tunneling current-voltage (I-V) curves of the nanocomposites measured below the $T_{\rm C}$ of NbC would be mixed with the contribution of the variable range hopping conduction of the carbon nanofiber matrix. According to the ratio of the electrical conductances obtained near to the origin of coordinate from the I-V characteristics curves of the tunneling junctions in superconducting states at 2 K and those in normal states at 12 K, the nontunneling current is evaluated to be about 12% of the full current. Above the superconducting transition temperature, the I-V characteristic of such junctions measured at 12 K exhibits a linear relationship because the NbC nanocrystals are in a normal state. The temperature dependence of I-V characteristics for the specimen pellet of the nanocomposites as shown in Fig. 5 reveals a sum tunneling effect of all kinds of tunneling junctions embedded in the carbon nanofiber matrix.

In summary, the electronic transport properties of NbC(C)-C nanocomposites fabricated by arc discharging Nb in a methane (CH$_4$) atmosphere have been investigated. NbC nanocrystals in a cubic shape encapsulated by carbon shells are dispersed in a nonmetallic carbon nanofiber matrix. DC susceptibility measurements of the nanocomposites indicate that the $T_{\rm C}$ of the NbC nanocrystals was 10.7 K. The temperature dependence of the electrical resistivity of the nanocomposites, dominated by the carbon nanofibers matrix in a temperature range between the critical temperature of NbC and 300 K, follows the Mott's $T^{-1/4}$ law because electrons are strongly localized. The electronic transport behavior of the specimen pellet is influenced by a magnetic field due to the breakdown of superconductivity of NbC nanocrystals. When the change of its electrostatic energy ΔE is far greater than the thermal energy at very low temperatures, an electron can be localized on an isolated NbC nanocrystal, leading to Coulomb Blockade. The electron can go from one nanocrystal to the other by a tunneling mechanism. A collective behavior of electron tunneling effect is confirmed by current-voltage characteristics in a three-dimensional case. The gap of NbC crystals is not observed, due to the partial suppression of surface superconductivity through the contact between NbC nanocrystals and the carbon shells.

[1] B. Abeles *et al.*, Phys. Rev. Lett. **35**, 247 (1975).

[2] P. Sheng, B. Abeles, and Y. Arie, Phys. Rev. Lett. **31**, 44 (1973).

[3] P. Sheng *et al.*, Phys. Rev. Lett. **40**, 1197 (1978).

[4] E. K. Sichel *et al.*, Phys. Rev. B **18**, 5712 (1978).

[5] B. Abeles *et al.*, Adv. Phys. **24**, 407 (1975).

[6] B. Abeles, in *Applied Solid State Science*, edited by R. Wolfe (Academic, New York, 1976), Vol. 6, pp. 1–117.

[7] S. T. Chui, Phys. Rev. B **43**, 14274 (1991).

[8] D. Toker *et al.*, Phys. Rev. B **68**, 041403(R) (2003).

[9] I. Balberg *et al.*, Int. J. Mod. Phys. B **18**, 2091 (2004).

[10] G. Deutscher, in *Percolation, Localization, and Superconductivity*, edited by A. M. Goldmanand S. A. Wolf, NATO Advanced Studies Institute Series B, Vol. 109 (Plenum, New York, 1984), p. 95, and references therein.

[11] D. Stauffer and A. Aharony, *Introduction to Percolation Theory* (Taylor & Francis, London, 1992).

[12] K. Chattopadhyay, V. Bhattacharya, and A. P. Tsai, Mater. Res. Soc. Symp. Proc. **703**, 535 (2002).

[13] R. A. Buhrman and W. P. Halperin, Phys. Rev. Lett. **30**, 692 (1971).

[14] H. Takayama, Prog. Theor. Phys. **48**, 758 (1972).

[15] H. R. Zeller and I. Giaever, Phys. Rev. **181**, 789 (1969).

[16] P. G. de Gennes and M. Tinkham, Physics (Long Island City, N.Y.) **1**, 107 (1964).

[17] R. Kubo, J. Phys. Soc. Jpn. **17**, 975 (1962).

[18] A. Kawabata and R. Kubo, J. Phys. Soc. Jpn. **21**, 1765 (1966).

[19] A. Kawabata, J. Phys. (Paris), Colloq. **38**, 2 (1977).

[20] R. Kubo *et al.*, Annu. Rev. Mater. Sci. **14**, 49 (1984).

[21] J. P. Hurault *et al.*, Phys. Rev. B **3**, 762 (1971).

[22] Y. Yosoda, J. Appl. Phys. **92**, 5494 (2002).

[23] I. Sternfeld *et al.*, Phys. Rev. B **71**, 064515 (2005).

[24] X. L. Dong *et al.*, Phys. Rev. B **60**, 3017 (1999).

[25] Z. D. Zhang *et al.*, Phys. Rev. B **64**, 024404 (2001).

[26] E. V. Pechen *et al.*, Physica C **235–240**, 2511 (1994).

[27] Y. S. Karimov and T. G. Utkina, JETP Lett. **51**, 528 (1990).

[28] L. Shi *et al.*, Carbon **43**, 195 (2005).

[29] F. Tuinstra and J. L. Koenig, J. Chem. Phys. **53**, 1126 (1970).

[30] N. F. Mott, Philos. Mag. **22**, 7 (1970).

[31] S. I. Krasnosvobodtsev *et al.*, J. Exp. Theor. Phys. **81**, 534 (1995).

[32] Y. Yosida and I. Oguro, J. Appl. Phys. **86**, 999 (1999).

[33] I. Giaever and H. R. Zeller, Phys. Rev. Lett. **20**, 1504 (1968).

[34] C. O. Hwang and M. Mascagni, J. Appl. Phys. **95**, 3798 (2004).

[35] M. Tinkham, in *Introduction to Superconductivity*, edited by B. Bayne and M. Gardner (McGraw-Hill, New York, 1975).

[36] P. J. M. van Bentum *et al.*, Phys. Rev. Lett. **60**, 369 (1988).